sustainability

MDPI

Article

Effects of Connected Autonomous Vehicles on the Energy Performance of Signal-Controlled Junctions

Yiqing Wen [1,2,3], Yibing Wang [4], Zhao Zhang [5], Jiaxin Wu [1,2,3], Liangxia Zhong [1,2,3], Markos Papageorgiou [1,6] and Pengjun Zheng [1,2,3,*]

1 Faculty of Maritime and Transportation, Ningbo University, Ningbo 315000, China
2 Collaborative Innovation Center of Modern Urban Traffic Technologies, Southeast University, Nanjing 211189, China
3 National Traffic Management Engineering & Technology Research Center, Ningbo University Sub-Center, Ningbo 315832, China
4 Institute of Intelligent Transportation Systems, Zhejiang University, Hangzhou 310058, China
5 School of Transportation Science and Engineering, Beihang University, Beijing 100191, China
6 Dynamic Systems and Simulation Laboratory, Technical University of Crete, 73100 Chania, Greece
* Correspondence: zhengpengjun@nbu.edu.cn

Abstract: This study proposes an optimal control method for connected autonomous vehicles (CAVs) through signalized intersections to reduce the energy consumption of mixed human-driven vehicles (HDVs) and CAV traffic. A real-time optimal control model was developed to optimize the trajectory of each CAV by minimizing energy consumption during the control period while ensuring traffic efficiency and safety. The control conditions of the CAVs were analyzed under different driving scenarios considering the impact of signal phase timing and preceding vehicles. Additionally, a method is proposed for CAVs to guide other vehicles directly and reduce the energy consumption of the entire signalized intersection. Simulation experiments using MATLAB and SUMO were conducted to evaluate the performance of the proposed method under various traffic conditions, such as different levels of saturation, market penetration rates (MPRs), and the green ratio. The performance was measured using average energy consumption and an average time delay. The results show that the proposed method can effectively reduce vehicle energy consumption without compromising traffic efficiency under various conditions. Moreover, under traffic saturation, the proposed method performs better at a high MPR and green ratio, especially at 40–60% MPR.

Keywords: connected autonomous vehicles; eco-driving method; optimal control; signalized intersections; consumption performance

Citation: Wen, Y.; Wang, Y.; Zhang, Z.; Wu, J.; Zhong, L.; Papageorgiou, M.; Zheng, P. Effects of Connected Autonomous Vehicles on the Energy Performance of Signal-Controlled Junctions. *Sustainability* **2023**, *15*, 5672. https://doi.org/10.3390/su15075672

Academic Editor: Juneyoung Park

Received: 21 February 2023
Revised: 19 March 2023
Accepted: 22 March 2023
Published: 23 March 2023

1. Introduction

Eco-driving is an emerging practice aimed at enhancing energy efficiency and curbing transport emissions. It involves optimizing vehicle operation by minimizing unnecessary stops, acceleration, and deceleration and maintaining a steady speed to reduce energy consumption, improve traffic mobility, and decrease emissions [1–3]. The advent of connected autonomous vehicles (CAV) is also seen as a promising development that will further facilitate eco-driving by providing more space and opportunities for its implementation.

In the future, the adoption of CAVs is expected to trigger significant transformations in the safety, accessibility, and traffic flow dynamics of road transportation. By harnessing the power of traffic sensing, data collection, analysis, and processing, CAVs can employ eco-driving strategies to minimize vehicle energy consumption, conserve resources, and enhance economic efficiency [4]. However, the development of effective traffic management and control mechanisms for CAVs on the road still presents a pressing challenge in the transportation sector.

Signalized intersections serve as critical nodes within the urban road network where the smooth transition of traffic between interrupted and uninterrupted flow is crucial. However, these intersections often cause traffic interruptions and delays. Implementing eco-driving control for CAVs at signalized intersections is, therefore, essential to mitigate the negative impact on vehicles and traffic flow.

Current research on eco-driving methods for connected autonomous vehicles (CAVs) at traffic signal intersections has primarily relied on rule-based control methods. These methods adjust the vehicle's longitudinal speed based on signal state information to enable it to pass through the intersection without unnecessary stops. For example, Jin et al. [5] developed a mathematical model that categorized intersection signal states into six situations and optimized the movement of a single vehicle upstream and downstream of the intersection. Similarly, Lu et al. [6] computed appropriate constant velocities for continuous signalized intersections and employed smooth trigonometric curves to represent velocity changes during acceleration and deceleration, ensuring seamless passage through the intersection. However, as traffic environments become more complex, rule-based control methods have limitations, and optimizing control methods are computationally intensive. Hence, research on eco-driving for connected autonomous vehicles at signalized intersections now focuses on establishing a comprehensive optimization model that considers multiple objectives, including safety and efficiency.

Dynamic eco-driving modeling is an integrated framework that includes input space models, fuel consumption models, vehicle dynamics models, optimization objectives, and impact analyses of the eco-driving system on road areas and traffic signal control strategies [7]. Optimal control methods are preferred due to their low computational complexity. Zhang et al. [8] proposed a constrained optimization model that approximates optimal results similar to the pseudo-spectral method. Cheng et al. [9] introduced a model-free control method based on the Monte Carlo search tree algorithm. Decentralized control strategies have been effective in improving road traffic efficiency while considering CAV eco-driving, such as the model proposed by Yao and Li [10], which minimizes vehicle travel time, fuel consumption, and safety risks.

The behavior of multiple CAVs at signalized intersections has a significant impact on the application of eco-driving. Hence, studying connected vehicle queues is critical to reducing traffic congestion, improving road capacity, and decreasing energy consumption. Jiang et al. [11] and Chen et al. [12] developed a system for multi-vehicle driving at signalized intersections by combining a microscopic vehicle-following model with optimal control methods. Zhang et al. [13] and Chen et al. [14] proposed vehicle emission row schemes and the concept of "1 + n" mixed platoon to enhance overall traffic efficiency and fuel consumption at intersections. Wang et al. [15] suggested that the front CAV's speed trajectory provides a reference for the rear vehicle, leading to effective energy savings. Xu and Deng [16] divided vehicles into fleets and calculated four speed guidance models to achieve optimal acceleration and deceleration and pass the signalized intersection at the same target speed as the lead vehicle. Various optimization control methods are employed in eco-driving research, including Pulse-and-Glide (PnG) cycle control [17], model predictive control (MPC) [18–20], deep learning algorithms [21–23], and optimal control [24,25]. However, most of these approaches are computationally intensive and challenging to apply to the centralized control of traffic flow at signalized intersections. It is worth noting that, although Rad S R et al. [26] proposed a conceptual framework for designing dedicated lanes for connected autonomous vehicles, it requires intelligent infrastructure, which may be challenging to implement. This paper proposes an optimal control method for CAVs at signalized intersections and a decentralized control strategy to mix traffic at existing signalized intersections, enabling CAVs to promote other environmentally friendly driving vehicles safely, smoothly, and indirectly, thus reducing total road energy consumption. The main contribution of our paper is to extend the optimal control method for intersections by considering mixed traffic flows and integrated energy consumption models. This method can be applied to mixed traffic flow and meet actual traffic conditions, and it can effectively

reduce the energy consumption of human-driven vehicle (HDV) and CAV mixed traffic while balancing traffic efficiency. Moreover, we comprehensively analyze the energy-saving potential of connected autonomous vehicles at signalized intersections.

The paper is divided into four main sections. The first section describes the scenario and motivation for the study. The second section proposes an optimal control method using optimal control theory. In the third section, simulations and analyses of the proposed method are presented. Finally, the last section concludes the research and summarizes the main findings.

2. Scenario Description

We consider a mixed traffic scenario at a typical signal-controlled intersection, as shown in Figure 1, where both HDVs and CAVs travel through the intersection in sequence. The intersection has fixed signal phase and timing (SPaT) information, and the signal is located at the center. To facilitate eco-driving, the intersection is divided into two areas based on previous research: the control zone and the merging zone. The control zone is where CAVs obtain SPaT and vehicle information, while the merging zone is the area within the green box line in the figure where the signals guide vehicles through the intersection.

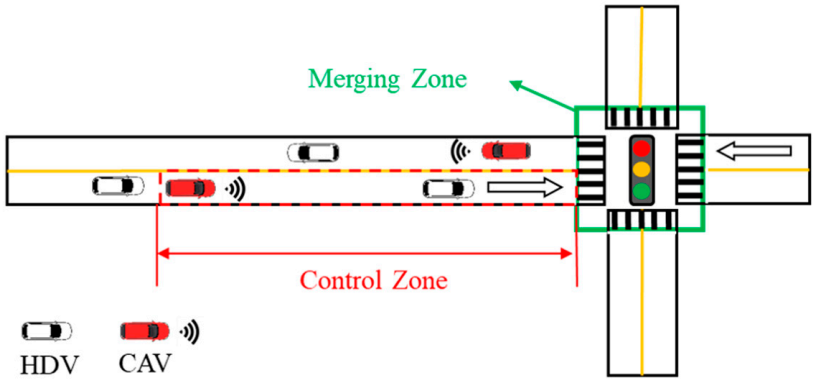

Figure 1. Illustration for the mixed traffic-signal-controlled junction.

Our study focused on optimizing the eco-driving of individual CAVs in a single-lane control zone at a signal-controlled intersection. We developed an optimal control method based on the vehicle's dynamics, initial and final states, and constraints to minimize energy consumption by optimizing the acceleration of the vehicle phase. Each CAV obtains relevant information for optimal control upon entering the control zone and controls its acceleration through the intersection accordingly. We also used the Intelligent Driver Model (IDM) [27] to model the trajectory of HDVs and follow them specifically. To facilitate information processing and calculations, we set the control zone distance as l and used the stop line as the origin.

Our control design and analysis for the signal-controlled junction are based on the following assumptions.

1. All CAVs are connected, meaning they can transmit their own and surrounding vehicle information through wireless communication with real-time communication between vehicles and infrastructure. Communication delays or packet loss are not considered.
2. All CAVs can drive independently and follow the speed trajectory specified by the intelligent decision and algorithm system upon entering the control zone. HDVs are assumed to behave ideally.
3. To optimize vehicle efficiency in the control zone, overtaking or lane changing is not allowed. Furthermore, the impact of other roads on vehicle travel is not considered.
4. All vehicles passing through the signalized intersection are fueled vehicles, and other traffic disturbances, such as pedestrians or non-motorized vehicles, are not taken into account.

3. Methodology

Our study proposes an eco-driving method for CAVs that considers various practical driving situations in the control zone. We first define the vehicle state upon entering the control zone and then discuss the specific conditions that CAVs may encounter in this area. Finally, we develop an optimal control model for CAVs based on defined objectives and constraints.

3.1. Dynamical Modeling

Acquiring vehicle state information is vital for dynamic modeling; however, these states are not easily obtained directly. Numerous studies have been conducted to describe vehicle dynamics and design estimators by integrating the Global Navigation Satellite System (GNSS) [28], Inertial Measurement Unit (IMU) [29,30], and cameras [31] for state estimation. To provide an overview of the state descriptions commonly used in these studies, we assume that there are N vehicles entering and leaving the control zone at a specific time, numbered in chronological order. The position of CAV i ($i \in$ N) at time t is represented as $x_i(t)$; the velocity at time t is denoted by $v_i(t)$; and the acceleration at time t is expressed as $\dot{v}_i(t) = u_i(t)$. The system state vector of CAV i is given by $X(t) = [x_i(t), v_i(t)]^T$, and the longitudinal dynamics can be represented in a second-order form, as follows:

$$\begin{aligned} \dot{x}_i(t) &= v_i(t) \\ \dot{v}_i(t) &= u_i(t) \end{aligned} \tag{1}$$

Then, the system equation of state for CAV i is modeled as $\dot{X}(t) = [v_i(t), u_i(t)]^T$.

3.2. Cost Function

Eco-driving for CAVs at signalized intersections should prioritize driving safety and not hinder traffic maneuverability, as established in previous research and practical considerations. With these factors in mind, the primary control objective of vehicle eco-driving at signal intersections is to minimize total energy consumption. The optimal control cost function for CAV i is defined as

$$F = \varphi(X(t_f)) + \int_{t_0}^{t_f} L(X(t), u(t))dt \tag{2}$$

where t_0 is the time when CAV i enters the control zone, i.e., reaches the boundary of control zone as shown in Figure 1, and the time for CAV i to reach the stop line is the final time, t_f, which will be discussed later in Section 3.4.

As the terminal cost function in Equation (2), $\varphi(X(t_f))$ represents the error between the vehicle and the desired state at the final time, which is expressed by Equation (3). The terminal cost ensures the CAV can enter the intersection on time at a preferred speed. Note that the stop line is set as the $x = 0$ position, and the first term of Equation (3) is expressed as the deviation of CAV i from $x = 0$ at the final time, t_f; the second term of Equation (3) is expressed as the deviation of CAV i from the desired velocity, v_i^d, at the final time, t_f. In Equation (3), ω_1, ω_2 are the penalty weighting coefficients for the position deviation and speed deviation, respectively, which ensure a constraint on the vehicle's final state. The discussion on the desired velocity at the final time is in Section 3.4.

$$\varphi(X(t_f)) = \omega_1(x_i(t_f) - 0)^2 + \omega_2(v_i(t_f) - v_i^d)^2 \tag{3}$$

In Equation (2), $L(X(t), u(t))$ is the operating cost, and the first term in Equation (4) indicates the immediate energy consumption of CAV i at time t. The second term is a term created considering the driving comfort of CAV i. The sharpness and duration of acceleration and deceleration of the vehicle have a significant effect on the fuel consumption of the vehicle. We chose to utilize the instantaneous fuel consumption model proposed by M.A.S. Kamal et al. [32] based on vehicle dynamics, which is suitable for conventional

vehicles. At the same time, we assume that all vehicles on the road are fuel-powered vehicles with the same construction and assembly. The energy consumption model is shown below:

$$L(X(t), u(t)) = f_i(t) + \frac{1}{2}u_i(t)^2 \tag{4}$$

and

$$\begin{aligned} f_i(t) &= f_i^{cruise} + f_i^{accel} \\ f_i^{cruise} &= a + b_1 \cdot v_i(t) + b_2 \cdot v_i^2(t) + b_3 \cdot v_i^3(t) \\ f_i^{accel} &= u_i(t) \cdot (c_1 + c_2 \cdot v_i(t) + c_3 \cdot v_i^2(t)), \end{aligned} \tag{5}$$

The model uses standard vehicle engine characteristics and records velocity and acceleration to gather fuel consumption data, which are then used to create fuel consumption estimation equations through curve fitting. In Equation (5), f_i^{cruise} is the energy consumption caused by CAV i when the speed is $v_i(t)$ at moment t, and f_i^{accel} is the additional energy consumption caused by CAV i when the acceleration is $u_i(t)$ at moment t. It is necessary to note that fuel consumption does not occur when a vehicle is decelerating. Additionally, fuel consumption is a constant value, a, when the vehicle is idle. The coefficients in the equation are determined through curve fitting, and their values can be found in Table 1.

Table 1. Values for the coefficients of the energy consumption model equation.

Coefficient	Value
a	0.1569
b_1	0.0245
b_2	-7.415×10^{-4}
b_3	5.975×10^{-5}
c_1	0.07224
c_2	0.09681
c_3	1.075×10^{-3}

3.3. Constraint Conditions

Previous studies have highlighted various constraints present in traffic conditions at signal-controlled junctions. These constraints include vehicle safety, kinematic, and control state constraints.

Vehicle safety constraints are a critical aspect of road traffic and typically involve maintaining a minimum safe spacing between vehicles to ensure stability and safety. In our study, the safety constraint is defined as the requirement for all CAVs to maintain a safe distance from the vehicle in front of them, and the distance between CAV i and preceding vehicle $i-1$ is $\Delta x_i(t)$. The safety constraint is described as

$$\Delta x_i(t) - L_{veh} \geq \Delta x_i^{safe}(t),\ t \in \left[t_0, t_f\right],\ i = 1, \cdots, n \tag{6}$$

where L_{veh} is the length of the vehicle, and $\Delta x_i^{safe}(t)$ is the safe vehicle distance for CAV i at moment t. The safe vehicle distance can be obtained from $\Delta x_i^{safe}(t) = v_i(t) \cdot t_{safe}$, where t_{safe} is the safe headway.

Next, we take into account vehicle kinematics and constrain vehicle control based on speed, acceleration, and comfort requirements at the signalized intersection.

1. The speed limit sets a maximum allowable speed for vehicles on the road, while the minimum speed is constrained by road conditions and the movement of vehicles.

$$v_{\max} \geq v_i(t) \geq v_{\min},\ t \in \left[t_0, t_f\right],\ i = 1, \cdots, n \tag{7}$$

2. We specify the safe maximum acceleration and maximum deceleration of the vehicle.

$$u_{\max} \geq u_i(t) \geq u_{\min},\ t \in \left[t_0, t_f\right],\ i = 1, \cdots, n \tag{8}$$

3. We consider maintaining the comfort of driving the vehicle and describe it as the rate of change in acceleration, $k_i(t) = \frac{\partial u_i(t)}{\partial t}$, which represents the rate of change in the acceleration of CAV i at moment t.

$$k_{\max} \geq k_i(t) \geq k_{\min},\ t \in \left[t_0, t_f\right],\ i = 1, \cdots, n \tag{9}$$

Last, regarding the vehicle control state constraint, the terminal state constraint has been bounded by the terminal cost, $\varphi(X(t_f))$, of Equation (2), and the initial state constraint, v_i^0, is the speed of CAV i at t_0, the initial moment; then, the initial state constraint is

$$x_i(t_0) = -lv_i(t_0) = v_i^0,\ i = 1, \cdots, n \tag{10}$$

3.4. Final Time and Desired Velocity

Upon entering the control zone for optimal control, the CAV must gather SPaT information and information on preceding vehicles to determine its desired velocity and the final time to reach the stop line. Previous studies [33] often set the desired velocity as the restricted velocity to ensure maximum traffic volume at intersections. However, this approach may not balance vehicle fuel consumption and traffic efficiency in practical situations.

Therefore, we analyzed the optimal final time, t_f, and desired velocity, v_i^d, of CAV i for various scenarios. The signal phase starts from the red phase at time $t = 0$, and the signal period is T_{cycle}. The red phase time is T_r, and the green phase time is T_g. We started by discussing the final time, as it is directly linked to the desired velocity. Assuming that CAV i arrives at the stop line at the maximum velocity, the earliest possible time to exit the control zone is t_f^e.

$$t_f^e = t_0 - \frac{x_i(t_0) + \left[\left(v_{\lim}^2 - v_i^2(t_0)\right)/2u_{\max}\right]}{v_{\lim}} + \frac{v_{\lim} - v_i(t_0)}{u_{\max}} \tag{11}$$

(1) Assuming that there are no vehicles in front of CAV i, the final time and desired speed of the CAV can be determined based on the signal state.

If the t_f^e is at the redlight phase with $0 \leq mod(t_f^e, T_{cycle}) \leq T_r$, CAV i must wait until the next greenlight phase to proceed, and the final time is the start time of that green phase, provided by

$$t_f = \left\lfloor \frac{t_f^e}{T_{cycle}} \right\rfloor T_{cycle} + T_r \tag{12}$$

If the t_f^e is at the green phase with $T_r < mod(t_f^e, T_{cycle}) < T_{cycle}$, CAV i can pass through in the current phase, and the final time is the earliest possible time, provided by $t_f = t_f^e$.

(2) If there are other vehicles ahead of CAV i, its final time and desired speed will be adjusted based on the preceding vehicles. Assuming that there are n preceding vehicles, CAV i can only exit the intersection once all of the preceding vehicles have left.

If the initial time is at the redlight phase with $0 \leq mod(t_0, T_{cycle}) \leq T_r$, the final time depends on whether all preceding vehicles can leave at the same greenlight phase. If all preceding vehicles can leave at the same greenlight phase, the final time is provided by $nt_{safe} < T_g$. If $0 \leq mod(t_f^e, T_{cycle}) < T_r + nt_{safe}$, the final time is provided by

$$t_f = \left\lfloor \frac{t_0}{T_{cycle}} \right\rfloor T_{cycle} + T_r + nt_{safe} \tag{13}$$

However, if the final time is not affected by the preceding vehicles with $T_r + nt_{safe} \leq mod(t_f^e, T_{cycle}) < T_{cycle}$, the final time is $t_f = t_f^e$. If preceding vehicles fail to cross the intersection all at once with $nt_{safe} \geq T_g$, CAV i must wait until the next green phase to cross, and the final time is provided by

$$t_f = \left\lceil \frac{t_0}{T_{cycle}} \right\rceil T_{cycle} + T_r + \left\lfloor \frac{nt_{safe} - T_g}{t_{safe}} \right\rfloor t_{safe} \tag{14}$$

If the initial time is at the green light phase with $T_r < mod(t_0, T_{cycle}) < T_{cycle}$, the final time must also be determined based on the preceding vehicles. All preceding vehicles can leave at once with $mod(t_0, T_{cycle}) + nt_{safe} \leq T_{cycle}$. If $0 \leq mod(t_f^e, T_{cycle}) \leq T_r$, the final time is provided by Equation (12). If $T_r < mod(t_f^e, T_{cycle}) < T_{cycle}$, the final time can be expressed as Equation (13). However, if the preceding vehicles cannot cross the intersection all at once with $mod(t_0, T_{cycle}) + nt_{safe} > T_{cycle}$, the final time is provided by

$$t_f = \left\lceil \frac{t_0}{T_{cycle}} \right\rceil T_{cycle} + T_r + \left\lfloor \frac{mod(t_0 + nt_{safe}, T_{cycle})}{t_{safe}} \right\rfloor t_{safe} \tag{15}$$

Based on the final time, the desired velocity through the junction is determined. If the final time is the earliest time, t_f^e, then the desired velocity is set to the limit velocity, and we have $v_i^d = v_{\lim}$. However, if the final time is later than the earliest time, the desired velocity should be lower than the limit velocity to better reflect the actual situation of CAV i passing through the junction:

$$v_i^d = \max\left\{ \frac{-x_i(t_0)}{t_f - t_0}, v_{\min} \right\} \tag{16}$$

3.5. Optimal Control Model

The optimal control model for CAV i in the control zone of a signal-controlled junction can be expressed as a nonlinear optimization problem:

$$F = \varphi(X(t_f)) + \int_{t_0}^{t_f} L(X(t), u(t))dt \tag{17}$$

subject to constraints (6)–(10).

To solve this problem, the CAV must first collect SPaT and traffic information and determine the initial and final states, including the final time and desired velocity. The optimal control problem can then be solved using the Gaussian pseudospectra method in GPOPS-II [34]. GPOPS-II transforms the continuous-time optimal control problem into a nonlinear programming problem (NLP) and uses an NLP solver to obtain the optimal control solution.

3.6. Control Method for Connected Automated Vehicle

We made the assumption that the CAV performs optimal control planning as soon as it enters the control zone and this planning process only occurs once. In fact, due to the low traffic flow and the low influence between vehicles, the eco-driving of the CAV is almost undisturbed. However, the traffic flow is constantly changing, and higher traffic flow can affect the normal driving of adjacent vehicles, thereby disturbing the eco-driving of the CAV.

When the CAV enters the control zone, we considered two scenarios. In the first scenario, if there is no vehicle in front of the CAV or if the CAV and the preceding vehicle meet the conditions stated in Equation (6), the CAV can perform optimal control and drive through the control zone according to the optimized trajectory. In the second scenario, if the CAV and the preceding vehicle do not meet the conditions in Equation (6), the CAV cannot

perform eco-driving and must follow the preceding vehicle through the signal intersection using the following model of HDV.

While driving through the control zone, the CAV continuously detects the safe headway from the preceding vehicle in real-time. If the safe headway is satisfied, the CAV follows the optimized trajectory until it leaves the intersection. However, if the CAV detects that it is not at a safe headway from the preceding vehicle, it interrupts the eco-driving and follows the preceding vehicle through the signal intersection using the following model of HDV.

Figure 2 illustrates the driving methods of CAVs in different states.

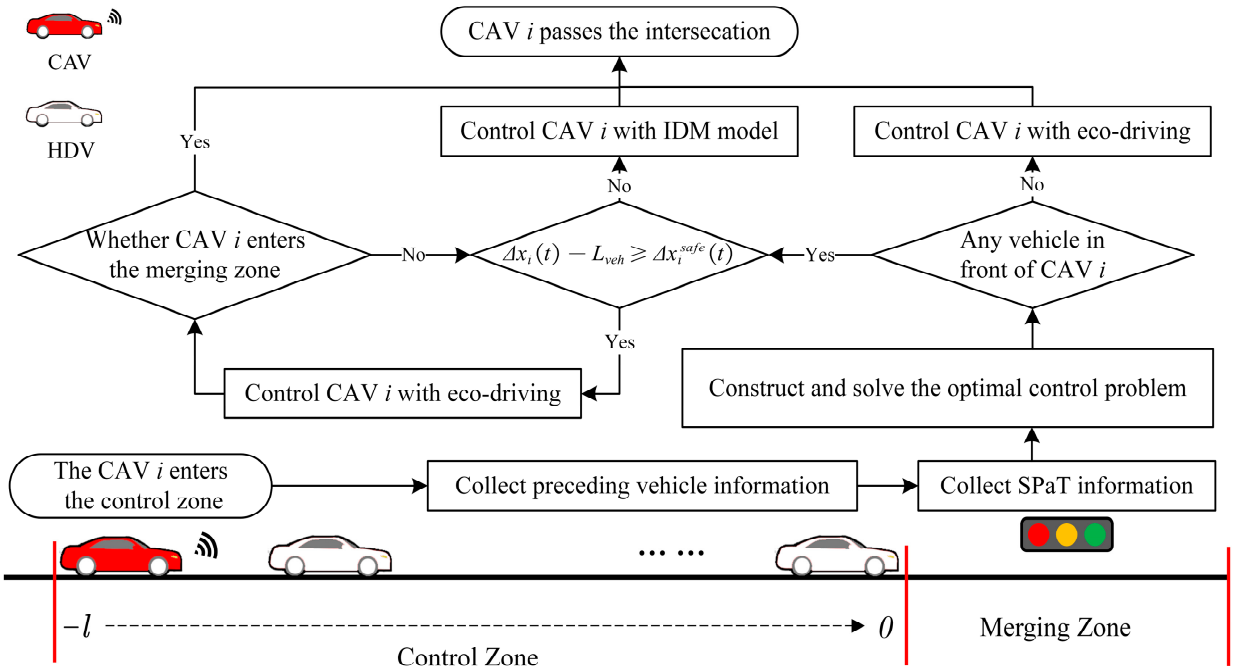

Figure 2. Illustration of the driving methods for CAVs at a signal-controlled junction.

4. Simulation Analysis

In this section, we conduct simulation experiments to assess the effectiveness of the proposed eco-driving method. The simulation environment setting and performance index of the experiment are introduced. Next, we analyze the simulation results of traffic flow trajectory in comparison to uncontrolled traffic flow trajectory. Finally, we compare and analyze the simulation results under varying saturation, MPR, and green ratio conditions.

4.1. Simulation Setting and Calculation

To evaluate the impact of CAVs on the energy performance of signal-controlled intersections, we performed joint simulations using MATLAB and the microsimulation software SUMO (Simulation of Urban Mobility) [35]. We designed experimental sets of flows with different MPRs and signal periods and analyzed the performance of a hypothetical signalized intersection scenario using the uncontrolled scenario as the baseline group.

4.1.1. Simulation Setting

To conduct the simulation, we established a single-lane, signal-controlled intersection in the SUMO simulation environment. The control zone was set to 300 m with a zero-gradient road segment. All vehicles were of the same size, with a length of 5 m, and exhibited random speeds while moving straight on the intersection following the Intelligent Driver Model (IDM) by default. The saturation flow rate of a single-lane road was set to 1830 veh/h, and the vehicle arrival pattern followed a Poisson distribution. This distribution assumes that the arrival of vehicles follows a random process, and the

probability of a certain number of vehicles arriving in a given time interval is determined by the mean arrival rate. We used this distribution to simulate the random arrival of vehicles at the intersection. We conducted intersection simulation experiments with different MPRs, traffic saturation levels, and green ratios in SUMO. The term "green ratio" referred to the proportion of time the traffic signal is green for a particular approach or direction compared with the entire traffic signal cycle time. The traffic saturation conditions were unsaturated (V/C = 0.6) and saturated (V/C = 1.0), and the green ratios were set to 0.3, 0.5, and 0.7. The parameters related to vehicle movement were mainly based on reference [33], and Table 2 shows some basic parameter settings for intersection and vehicle simulation.

Table 2. Simulation parameter settings.

Parameter	Symbol	Value
Simulation step (s)	T_s	0.2
Control zone (m)	l	300
Signal cycle (s)	T_{cycle}	60
Maximum acceleration (m/s^2)	$u_{\max}$	3
Maximum deceleration (m/s^2)	$u_{\min}$	4
Velocity limit (km/h)	$v_{\lim}$	60
Minimum velocity (km/h)	$v_{\min}$	10
Safe time headway (s)	t_{safe}	1.6
Weight coefficients of position deviation	ω_1	10
Weight coefficients of speed deviation	ω_2	100

Optimal control was carried out in MATLAB, and the driving state information of the CAV in SUMO was obtained in real-time through TraCI (Traffic Control Interface) as the input to the optimal control model. We used GPOPS-II (General-Purpose Optimal Control Software-II) to solve the model and obtain the optimal trajectory of the control zone, including the vehicle position, velocity, and acceleration. Some parameters in GPOPS-II are shown in Table 3. Finally, the optimal driving trajectory was sent to SUMO as the output of the CAV optimal control, and the CAV followed the optimized trajectory until it left the signalized intersection.

Table 3. Parameters of GPOPS.

Parameter	Value
setup. nlp. solver	snopt
setup. derivatives. supplier	sparseCD
setup. derivatives. derivativelevel	second
setup. mesh. method	hp1
setup. mesh. tolerance	10^{-3}
setup. mesh. maxiteration	10
setup. method	RPMintegration

4.1.2. Performance Index

Previous eco-driving assessment studies have evaluated the ecological impact of vehicles using metrics such as vehicle emissions and pollutant volumes, which are directly related to vehicle energy consumption and calculated using energy consumption and emissions models [36–38]. However, in this study, we focused primarily on fuel consumption as the main evaluation factor. To estimate the fuel consumption of each vehicle, we utilized the fuel consumption estimation model, $f_i(t)$, in Equation (5) and analyzed the average energy consumption performance.

In addition to evaluating vehicle energy consumption, we also considered intersection traffic efficiency as an important factor. In fact, CAV movements at signal-controlled intersections cannot affect the traffic efficiency of the traffic flow. The impact of CAV

movements on traffic efficiency at signal-controlled intersections was assessed by analyzing the average travel time delay (ATTD) of all vehicles, as shown in Equation (18).

$$ATTD = \frac{1}{n}\sum_{i=0}^{n}\left(T_i - \frac{l}{v_{\lim}}\right) \quad (18)$$

where T_i is the total travel time of vehicle i in the signal intersection area. If the time for each vehicle on the road is $\frac{l}{v_{\lim}}$, the vehicles pass through the intersection area in free flow.

4.2. Simulation Results and Discussion

4.2.1. Comparison against Non-Controlled Trajectory

The simulation results compared the trajectories of traffic flow with different MPRs and saturations at signalized intersections, with a basic control group consisting of all vehicles being HDVs and no eco-driving control being applied.

The spatiotemporal diagram of the simulated traffic flow trajectory under different saturations and MPRs is presented in Figure 3, where the green ratio is 0.5. In the spatiotemporal trajectory diagram, the red horizontal line represents the phase of the signal control red light, the blue dashed line represents the trajectory of the HDV, and the pink solid line represents the trajectory of the CAV for eco-driving. It was found that the impact of CAV eco-driving on traffic flow at intersections depends on the MPR and saturation levels. Figure 3a shows the traffic flow trajectory under the unsaturated condition. When the MPR is $\leq$ 40% for eco-driving, the CAV has a significant impact on the traffic flow at the intersection. Figure 3b shows the traffic flow trajectory under saturation conditions. It can be found that under the same MPR condition, CAV intervention had a greater impact on traffic flow at the intersection under the saturated condition. Because the traffic flow runs relatively smoothly under unsaturated conditions, CAVs for eco-driving have a limited impact on the traffic flow at signalized intersections.

Compared with uncontrolled vehicles, CAV eco-driving can avoid queuing and idling during the redlight phase, leading to a smoother driving track and reduced energy consumption. With an improved MPR, CAV eco-driving can also guide the driving track of nearby vehicles, resulting in a smoother and more efficient traffic flow at the signalized intersection. The impact of traffic shock waves generated by congestion can also be reduced with higher MPRs. Overall, the simulation results demonstrate the effectiveness of the proposed eco-driving method in improving energy consumption and traffic efficiency at signal-controlled intersections.

4.2.2. Performance Evaluation and Analysis under Different Saturations, MPRs, and Green Ratios

The performance of the proposed method was evaluated and analyzed under different levels of saturation, MPRs, and green signal ratios. Average fuel consumption and travel time delay were used as performance indicators, and an uncontrolled traffic flow (MPR = 0%) group was selected as a baseline for evaluation.

To determine the impact of the proposed method on traffic efficiency, the average travel time delay of the traffic flow was analyzed. Results from Table 4 show that under increasing saturation, the average travel time delay increases in the control area, while under saturated conditions, the delay decreases with increasing MPRs and green signal ratios. Figure 4 illustrates the average travel time delay results of traffic flow in the control area at varying saturation levels during the simulation. Under the unsaturated condition (V/C = 0.6), the ATTD was not significantly impacted by the increase in the MPR because vehicles at the intersection could be released smoothly at this time. In contrast, under saturation conditions (V/C = 1.0), the proposed method resulted in decreased average travel time delay, indicating improved intersection traffic efficiency. Furthermore, shorter green ratios led to longer travel time delays for vehicles, but the intervention of CAVs reduced the delay by guiding HDVs to follow a smoother path. Overall, the proposed

method improved intersection traffic efficiency and reduced travel time delays, particularly under saturated conditions with low green signal ratios.

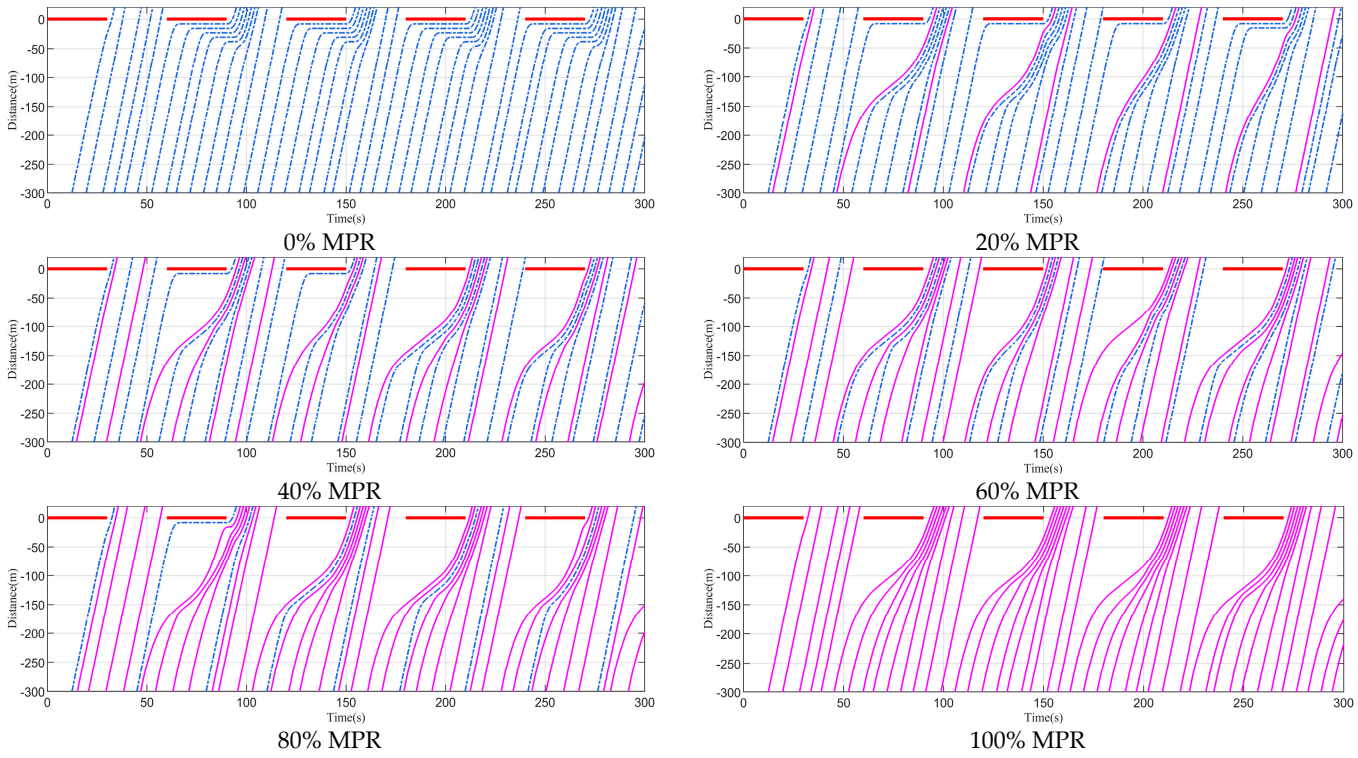

(**a**)

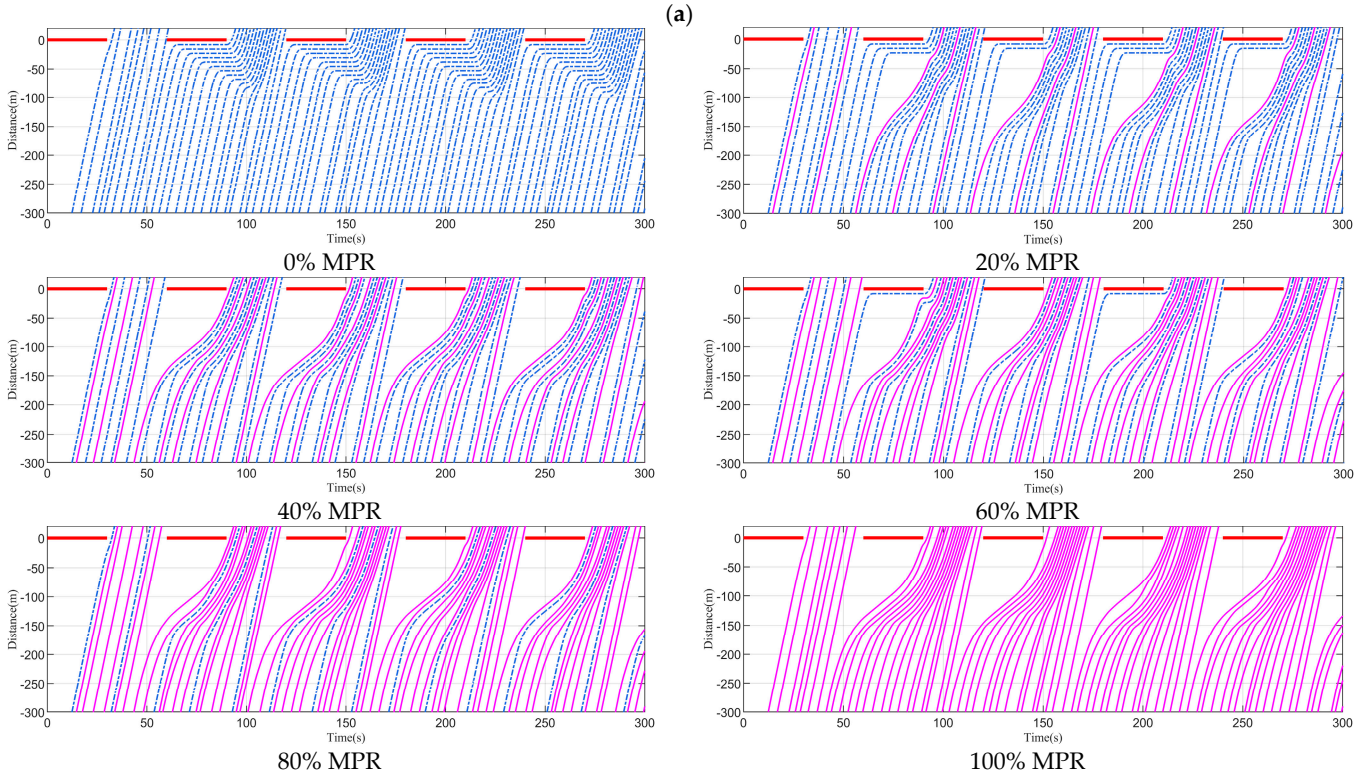

(**b**)

Figure 3. Vehicle trajectories of different MPRs at signalized intersections (the green ratio is 0.5). The blue dashed dot lines represent HDVs' trajectories, while the pink solid lines represent the CAVs' trajectories. (**a**) V/C = 0.6; (**b**) V/C = 1.0.

Table 4. Average travel time delay (s) simulation results of 0–100% MPRs under different green ratios and saturation levels.

Green Ratio	Saturation(V/C)	MPR					
		0%	20%	40%	60%	80%	100%
0.3	0.6	17.86	18.33	18.23	18.43	18.72	16.44
	1.0	43.65	26.81	25.22	26.88	20.48	21.51
0.5	0.6	10.43	10.10	10.02	10.14	10.08	10.34
	1.0	14.74	13.68	12.78	12.15	12.72	13.30
0.7	0.6	4.08	4.00	3.77	3.72	3.92	3.95
	1.0	8.49	7.21	7.04	7.65	7.52	6.13

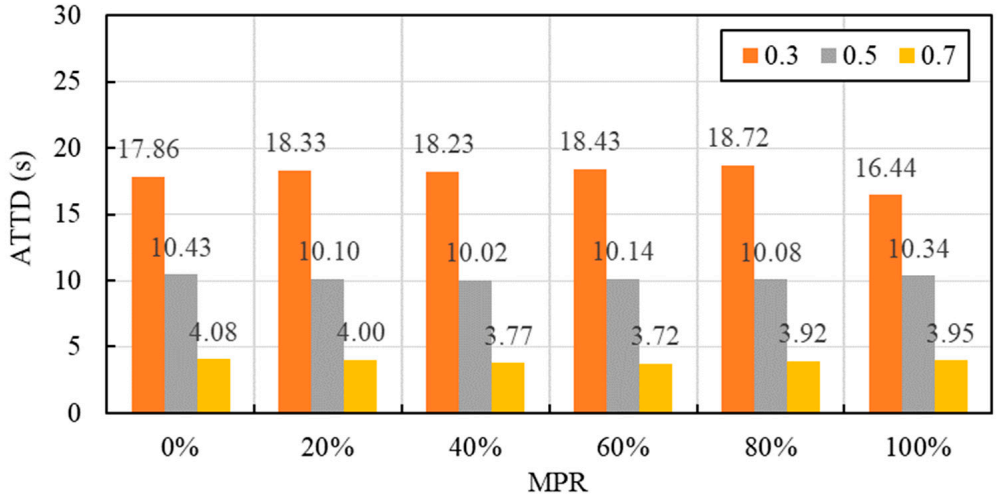

(**a**)

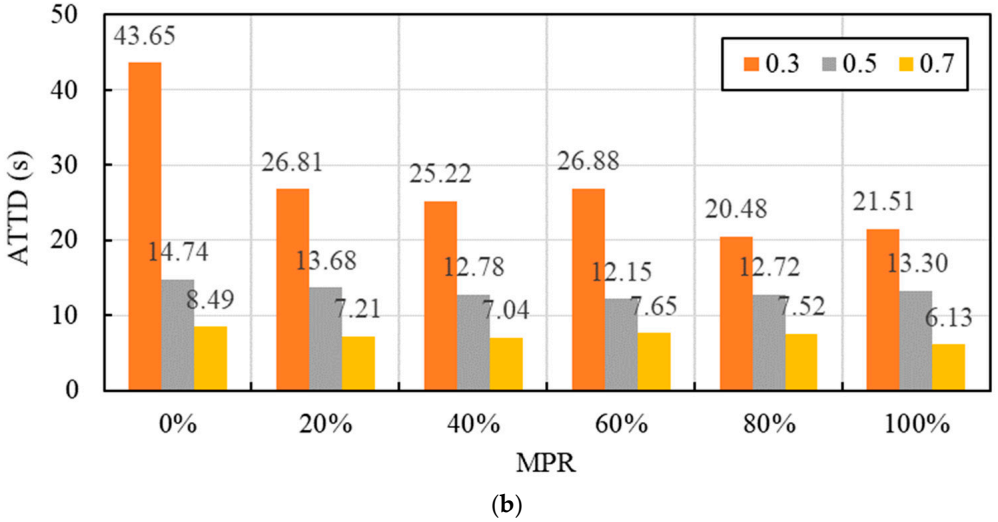

(**b**)

Figure 4. Average travel time delay of simulation results. (**a**) V/C = 0.6; (**b**) V/C = 1.0.

Furthermore, the average energy consumption results under different MPRs and green ratios at two saturation levels are presented in Figure 5 and Table 5. The blue, black, and pink lines in Figure 5 represent green ratios of 0.3, 0.5, and 0.7, respectively, while the dotted and solid lines indicate saturation levels of 0.6 and 1.0, respectively. The results show that the energy consumption decreases significantly with the increase in the green signal ratio for all HDVs, and the energy consumption is higher at V/C = 1.0 than at V/C = 0.6. More vehicles and shorter green times significantly increase road energy consumption, which is

consistent with actual traffic conditions at signalized intersections. Moreover, under the same saturation condition, the average energy consumption decreases with the increase in the MPR compared with the uncontrolled results. Under the same MPR condition, the energy consumption optimization benefit under saturation conditions is higher than under unsaturated conditions. The increase in the signal green ratio effectively reduces idle time and significantly reduces the average energy consumption of the traffic flow. Compared with the uncontrolled results, all the elevated MPR and green ratio conditions had significant energy efficiency benefits.

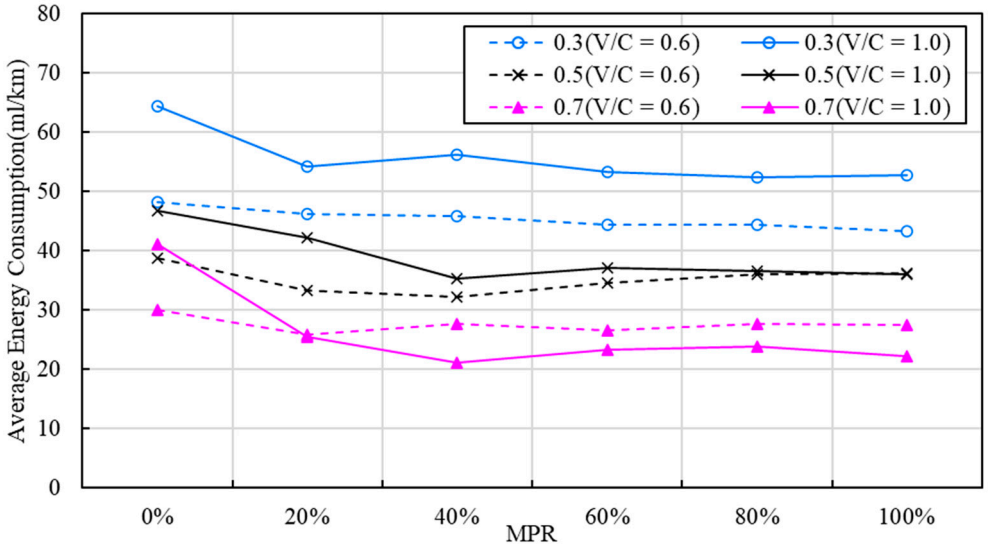

Figure 5. Average energy consumption (ml/km) across different scenarios with green ratios of 0.3, 0.5, and 0.7 and saturation levels of 0.6 and 1.0.

Table 5. Average energy consumption (ml/km) simulation results of 0–100% MPRs under different green ratios and saturations.

Green Ratio	Saturation(V/C)	MPR					
		0%	20%	40%	60%	80%	100%
0.3	0.6	48.31	46.25	45.84	44.37	44.32	43.25
	1.0	64.43	54.21	56.21	53.35	52.46	52.78
0.5	0.6	38.80	35.94	37.48	35.26	36.59	36.27
	1.0	46.80	42.30	35.35	37.13	36.56	35.96
0.7	0.6	30.04	25.85	27.65	26.63	27.67	27.40
	1.0	41.16	25.41	21.21	23.29	23.79	22.28

To further analyze the improvement effect of the proposed method on energy consumption, Figure 6 illustrates the degree of improvement in the average energy consumption of the traffic flow under different saturation levels compared to the uncontrolled results. Figure 6a shows that the energy consumption benefit under saturated conditions (V/C = 1.0) is significantly higher than under unsaturated conditions (V/C = 0.6) under the same conditions. This is due to the larger traffic flow and more HDVs affected by CAV driving under saturated conditions, and the intersection under unsaturated conditions can evacuate all vehicles quickly. Additionally, the analysis of the impact of the MPR indicates that the improvement of the CAV at the intersection is not significantly positively correlated with the increase in MPR. Figure 6b, under saturated conditions, shows that the eco-driving of a CAV can significantly affect the average energy consumption at the intersection when the MPR is lower than 40%, and the decreasing trend of average energy consumption becomes slow with the increase in the MPR level. The results of the study

indicate that the impact of the MPR on intersection energy consumption is similar for unsaturated conditions, while for saturated conditions, the greatest improvement occurs at a 40–60% MPR. This suggests that the proposed method is effective at a low MPR and has the potential to be applied to real traffic. Furthermore, with the increase in the signal green ratio, the eco-driving of CAVs becomes more significant in reducing energy consumption. Specifically, as the green ratio increases, the average energy consumption of traffic flow further decreases due to the eco-driving of CAVs. This effect is particularly pronounced when the green ratio is 0.7 and the MPR is 40% under saturated conditions, where the maximum optimization degree of energy consumption reaches 48.46%. This could be attributed to the fact that the eco-driving behavior of CAVs affects more HDVs in the passing phase, leading to a more significant reduction in energy consumption.

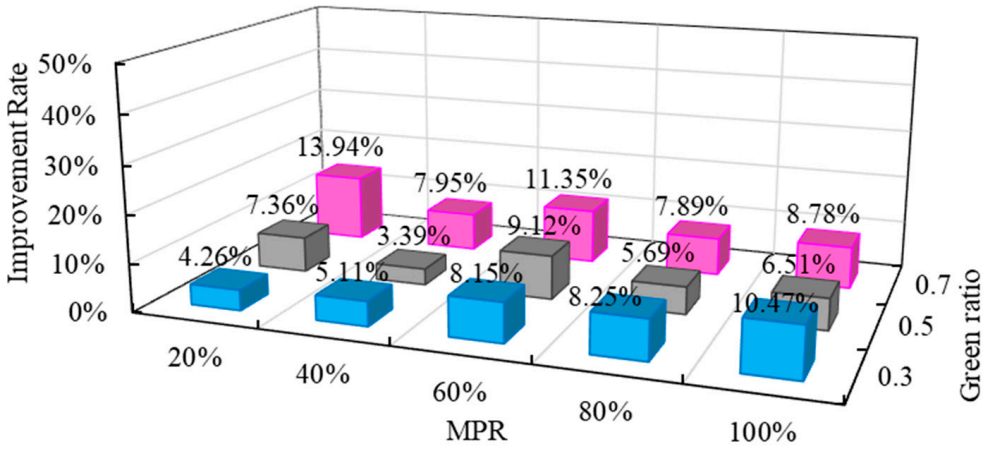

(**a**)

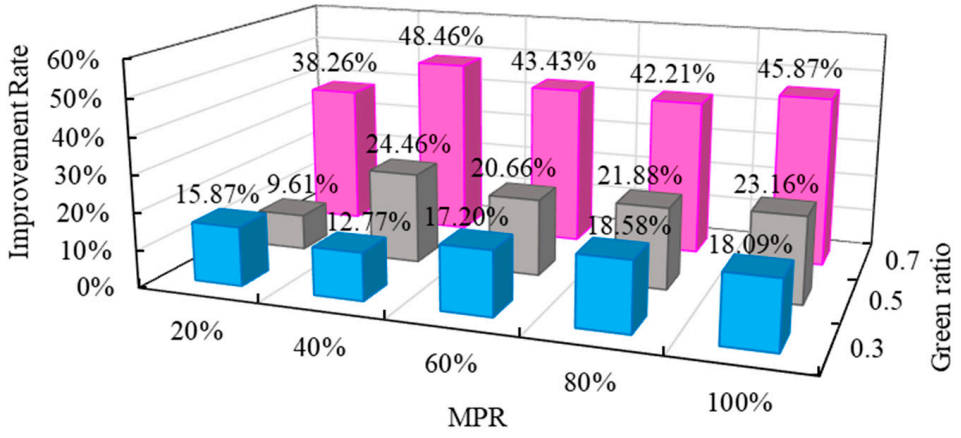

(**b**)

Figure 6. Average energy consumption improvement of simulation results. The reference value of 0% MPR is selected as the assessment baseline. (**a**) V/C = 0.6; (**b**) V/C = 1.0.

4.2.3. Comparison with GlidePath

The proposed method was compared with the GlidePath method developed by the Federal Highway Administration (FHWA) under the same simulation conditions. In the GlidePath method, the vehicle accelerates or decelerates to cruising speed in the shortest time and passes through intersections during green phases [39]. For ease of comparison, this section presents the average energy consumption and average travel time delay results of both methods under saturation conditions, which demonstrate the significant advantage of the proposed method in reducing energy consumption.

Table 6 presents a comparison of the average travel time delay results for both the proposed method and the GlidePath method. Under saturation conditions, both methods can ensure intersection traffic efficiency. As the MPR level increases, both methods are capable of reducing the travel time delay of vehicles at intersections to some extent under different green ratios. This demonstrates that the proposed method can offer the same advantages as the GlidePath system in terms of traffic efficiency.

Table 6. Average travel time delay (s) simulation results for the proposed method and GlidePath method.

Green Ratio	Method	MPR					
		0%	20%	40%	60%	80%	100%
0.3	Proposed method	43.65	26.81	25.22	26.88	20.48	21.51
	GlidePath	43.65	38.08	24.92	22.33	22.43	20.03
0.5	Proposed method	14.74	13.68	12.78	12.15	12.72	13.30
	GlidePath	14.74	14.24	12.87	13.33	13.28	14.56
0.7	Proposed method	8.49	7.21	7.04	7.65	7.52	6.13
	GlidePath	8.49	6.02	7.51	6.88	5.58	5.30

Table 7 presents a comparison of the two methods in terms of average energy consumption. The energy-saving advantage of the proposed method over GlidePath increases with an increase in MPR, particularly when MPR = 100%. As the green ratio increases, the proposed method has more potential for energy savings compared with GlidePath. Figure 7 shows a significant difference in the average energy consumption of GlidePath and the proposed method. The reason for this difference could be that the primary objective of the GlidePath is to improve maneuverability, which may lead to more shock waves in mixed traffic flow, thus reducing the energy-saving effect [33,40]. On the other hand, the proposed method enables CAVs to accelerate or decelerate smoothly, effectively guiding the eco-driving of other vehicles on the road and ensuring overall traffic efficiency while reducing energy consumption. Therefore, the proposed method has more potential for energy savings in mixed traffic flows.

Table 7. Average energy consumption (ml/km) simulation results for the proposed method and GlidePath method.

Green Ratio	Method	MPR					
		0%	20%	40%	60%	80%	100%
0.3	Proposed method	64.43	54.21	56.21	53.35	52.46	52.78
	GlidePath	64.43	59.09	56.93	54.91	55.42	55.85
0.5	Proposed method	46.80	42.30	35.35	37.13	36.56	35.96
	GlidePath	46.80	44.54	43.88	44.43	45.10	45.59
0.7	Proposed method	41.16	25.41	21.21	23.29	23.79	22.28
	GlidePath	41.16	36.29	37.21	38.97	36.31	37.14

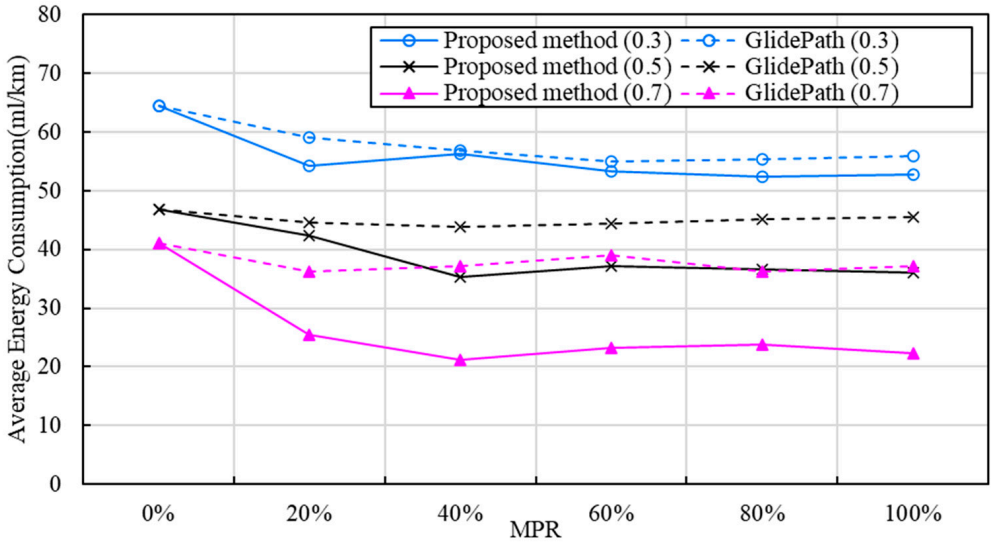

Figure 7. Average energy consumption (ml/km) results at green ratios of 0.3, 0.5, and 0.7.

5. Conclusions

This paper proposed an eco-driving method for CAVs in signalized intersections. When the CAV enters the control zone, it collects SPaT information and makes driving decisions. The eco-driving control in the control zone is determined based on a cost function derived from the vehicle dynamics model, and an optimal control model is constructed according to constraints. The optimal control problem is solved using GPOPS-II, and the CAV passed through the signalized intersection according to the optimal trajectory.

Simulation results were compared and analyzed under different conditions, including varying saturation levels, MPRs, and green ratios. The results demonstrate that the eco-driving method can smooth CAV trajectories, reduce the number of vehicle stops, and guide following vehicles more effectively. Compared with uncontrolled traffic flow, the intervention of CAVs at signalized intersections can improve energy efficiency without affecting traffic efficiency. Under unsaturated conditions (V/C = 0.6), a CAV has a weak effect on the ATTD and average energy consumption, as the intersection can fully release the vehicles on the road. However, under saturated conditions (V/C = 1.0), the eco-driving method can reduce the ATTD to a certain extent and significantly reduce energy consumption. The study also found that increasing the green ratio and MPR can improve energy consumption efficiency by more than 40%. In addition, a larger green ratio and a CAV permeability of 40–60% can guide other vehicles to achieve stable eco-driving, further improving the overall fuel consumption efficiency of the road.

While the research in this paper focused on a single lane at a single signal intersection with a mix of HDVs and CAVs, future studies will consider multi-lane driving and more complex traffic environments, such as lane changes and turning. The impact of multiple consecutive signal intersections on CAV eco-driving will also be studied to establish a more realistic eco-driving method.

Overall, this paper provides valuable insights into the potential benefits of eco-driving for CAVs at signalized intersections and highlights the need for further research in this area to fully consider the complexities of real-world traffic environments.

Author Contributions: Conceptualization, Y.W. (Yiqing Wen) and P.Z.; methodology, Y.W. (Yiqing Wen), Z.Z. and M.P.; software, Y.W. (Yiqing Wen), J.W. and L.Z.; validation, Y.W. (Yibing Wang), Z.Z. and P.Z.; formal analysis, M.P.; investigation, Y.W. (Yibing Wang); resources, P.Z.; writing—original draft preparation, Y.W. (Yiqing Wen); writing—review and editing, P.Z.; visualization, Y.W. (Yiqing Wen); supervision, M.P. and P.Z.; project administration, P.Z.; funding acquisition, P.Z. All authors have read and agreed to the published version of the manuscript.

Funding: This research was supported in part by the National Key Research and Development Program of China (2017YFE0194700), the National Natural Science Foundation of China (52272334, 61074142), the EC H2020 Project (690713), and the Zhejiang Natural Science Foundation (LY15E080013).

Institutional Review Board Statement: Not applicable.

Informed Consent Statement: Not applicable.

Data Availability Statement: Not applicable.

Acknowledgments: We would like to thank the National "111" Centre on Safety and Intelligent Operation of Sea Bridges (D21013), the Zhejiang 2011 Collaborative Innovation Center for Port Economy, and the Donghai Academy of Ningbo University for financial support in publishing this paper. The authors would like to thank the K.C. Wong Magna Fund at Ningbo University for sponsorship.

Conflicts of Interest: The authors declare no conflict of interest.

References

1. Barth, M.; Boriboonsomsin, K. Energy and emissions impacts of a freeway-based dynamic eco-driving system. *Transp. Res. Part D Transp. Environ.* **2009**, *14*, 400–410. [CrossRef]
2. Ding, F.; Jin, H. On the optimal speed profile for eco-driving on curved roads. *IEEE T Intell. Transp.* **2018**, *19*, 4000–4010. [CrossRef]
3. Lois, D.; Wang, Y.; Boggio-Marzet, A.; Monzon, A. Multivariate analysis of fuel consumption related to eco-driving: Interaction of driving patterns and external factors. *Transp. Res. Part D Transp. Environ.* **2019**, *72*, 232–242. [CrossRef]
4. Yang, L.; Zhao, X.; Wu, G.; Xu, Z.; Barth, M.; Hui, F.; Hao, P.; Han, M.; Zhao, Z.; Fang, S.; et al. Review on connected and automated vehicles based cooperative eco-driving strategies. *J. Traffic Transp. Eng.* **2020**, *20*, 58–72.
5. Jin, Q.; Song, G.; Ye, M.; Liu, J.; Yu, L. Optimization of eco-driving trajectories at intersections for energy saving and emission reduction. *Saf. Environ. Eng.* **2015**, *22*, 75–82.
6. Lu, Y.; Xu, X.; Ding, C.; Lu, G. Connected autonomous vehicle speed control at successive signalized intersections. *J. Beijing Univ. Aeronaut. Astronaut.* **2018**, *44*, 2257–2266.
7. Mintsis, E.; Vlahogianni, E.I.; Mitsakis, E. Dynamic eco-driving near signalized intersections: Systematic review and future research directions. *J. Transp. Eng. Part A Syst.* **2020**, *146*, 04020018. [CrossRef]
8. Zhang, X.D.; Zhang, T.; Zou, Y.; Du, G.D.; Guo, N.Y. Predictive eco-driving application considering real-world traffic flow. *IEEE Access* **2020**, *8*, 82187–82200. [CrossRef]
9. Cheng, Y.; Hu, X.; Tang, Q.; Qi, H.; Yang, H. Monte carlo tree search-based mixed traffic flow control algorithm for arterial intersections. *Transp. Res. Rec. J. Transp. Res. Board* **2020**, *2674*, 167–178. [CrossRef]
10. Yao, H.; Li, X. Decentralized control of connected automated vehicle trajectories in mixed traffic at an isolated signalized intersection. *Transp. Res. Part C Emerg. Technol.* **2020**, *121*, 102846. [CrossRef]
11. Jiang, H.; An, S.; Wang, J. Spatial-temporal trajectory optimization control system for connected and automated vehicles at signalized intersections. *Sci. Technol. Eng.* **2018**, *18*, 162–168.
12. Chen, Z.; Luo, L. Speed trajectory optimization of connected autonomous vehicles at signalized intersections. *J. Transp. Inf. Saf.* **2021**, *39*, 92–98+156.
13. Zhang, J.; Dong, S.Y.; Li, Z.B.; Ran, B.; Li, R.; Wang, H. An eco-driving signal control model for divisible electric platoons in cooperative vehicle-infrastructure systems. *IEEE Access* **2019**, *7*, 83277–83285. [CrossRef]
14. Chen, C.Y.; Wang, J.W.; Xu, Q.; Wang, J.Q.; Li, K.Q. Mixed platoon control of automated and human-driven vehicles at a signalized intersection: Dynamical analysis and optimal control. *Transp. Res. Part C Emerg. Technol.* **2021**, *127*, 103138. [CrossRef]
15. Wang, H.L.; Peng, P.; Huang, Y.J.; Tang, X.L. Model predictive control-based eco-driving strategy for cav. *IET Intell. Transp. Syst.* **2019**, *13*, 323–329. [CrossRef]
16. Xu, L.; Deng, M. A speed guidance method at signalized intersections based on vehicle infrastructure cooperation. *J. Transp. Inf. Saf.* **2021**, *39*, 78–86.
17. Li, S.E.; Li, R.; Wang, Z.; Zhang, X.; Chen, H.; Xin, Z. Optimal periodic control of connected multiple vehicles with heterogeneous dynamics and guaranteed bounded stability. *IEEE Intell. Transp. Syst.* **2020**, *12*, 110–124. [CrossRef]
18. Kamal, M.A.S.; Mukai, M.; Murata, J.; Kawabe, T. Model predictive control of vehicles on urban roads for improved fuel economy. *IEEE Transport. Contr. Syst. T* **2013**, *21*, 831–841. [CrossRef]
19. Wang, Y.; Liu, Z.; Zuo, Z.; Li, Z.; Wang, L.; Luo, X. Trajectory planning and safety assessment of autonomous vehicles based on motion prediction and model predictive control. *IEEE Trans. Veh. Technol.* **2019**, *68*, 8546–8556. [CrossRef]
20. Dixit, S.; Montanaro, U.; Dianati, M.; Oxtoby, D.; Mizutani, T.; Mouzakitis, A.; Fallah, S. Trajectory planning for autonomous high-speed overtaking in structured environments using robust mpc. *IEEE T Intell. Transp.* **2020**, *21*, 2310–2323. [CrossRef]
21. Wu, Z.Y.; Qiu, K.; Gao, H.B. Driving policies of v2x autonomous vehicles based on reinforcement learning methods. *IET Intell. Transp. Syst.* **2020**, *14*, 331–337. [CrossRef]

22. Liu, X.; Liu, Y.; Chen, Y.; Hanzo, L. Enhancing the fuel-economy of v2i-assisted autonomous driving, a reinforcement learning approach. *Trans. Veh. Technol.* **2020**, *69*, 8329–8342. [CrossRef]
23. Lee, H.; Kim, N.; Cha, S.W. Model-based reinforcement learning for eco-driving control of electric vehicles. *IEEE Access* **2020**, *8*, 202886–202896. [CrossRef]
24. Hoogendoorn, S.; Hoogendoorn, R.; Wang, M.; Daamen, W. Modeling driver, driver support, and cooperative systems with dynamic optimal control. *Transp. Res. Rec.* **2012**, *2316*, 20–30. [CrossRef]
25. Zhao, J.; Knoop, V.L.; Wang, M. Two-dimensional vehicular movement modelling at intersections based on optimal control. *Transp. Res. Part B Methodol.* **2020**, *138*, 1–22. [CrossRef]
26. Rad, S.R.; Farah, H.; Taale, H.; van Arem, B.; Hoogendoorn, S.P. Design and operation of dedicated lanes for connected and automated vehicles on motorways: A conceptual framework and research agenda. *Transp. Res. Part C Emerg. Technol.* **2020**, *117*, 102664.
27. Treiber, M.; Kesting, A. *Traffic Flow Dynamics: Data, Models and Simulation*; Springer: Cham, Switzerland, 2013.
28. Xia, X.; Hashemi, E.; Xiong, L.; Khajepour, A. Autonomous vehicle kinematics and dynamics synthesis for sideslip angle estimation based on consensus kalman filter. *IEEE Trans. Control. Syst. Technol.* **2023**, *31*, 179–192. [CrossRef]
29. Xiong, L.; Xia, X.; Lu, Y.S.; Liu, W.; Gao, L.T.; Song, S.H.; Yu, Z.P. Imu-based automated vehicle body sideslip angle and attitude estimation aided by gnss using parallel adaptive kalman filters. *IEEE Trans. Veh. Technol.* **2020**, *69*, 10668–10680. [CrossRef]
30. Liu, W.; Xia, X.; Xiong, L.; Lu, Y.S.; Gao, L.T.; Yu, Z.P. Automated vehicle sideslip angle estimation considering signal measurement characteristic. *IEEE Sens. J.* **2021**, *21*, 21675–21687. [CrossRef]
31. Liu, W.; Xiong, L.; Xia, X.; Lu, Y.S.; Gao, L.T.; Song, S.H. Vision-aided intelligent vehicle sideslip angle estimation based on a dynamic model. *IET Intell. Transp. Syst.* **2020**, *14*, 1183–1189. [CrossRef]
32. Kamal, M.A.S.; Mukai, M.; Murata, J.; Kawabe, T. Ecological vehicle control on roads with up-down slopes. *IEEE Trans. Intell. Transp. Syst.* **2011**, *12*, 783–795. [CrossRef]
33. Jiang, H.; Hu, J.; An, S.; Wang, M.; Park, B.B. Eco approaching at an isolated signalized intersection under partially connected and automated vehicles environment. *Transp. Res. Part C Emerg. Technol.* **2017**, *79*, 290–307. [CrossRef]
34. Patterson, M.A.; Rao, A.V. Gpops-ii: A matlab software for solving multiple-phase optimal control problems using hp-adaptive gaussian quadrature. *ACM Trans. Math. Softw.* **2014**, *41*, 1–37. [CrossRef]
35. Lopez, P.A.; Behrisch, M.; Bieker-Walz, L.; Erdmann, J.; Flotterod, Y.-P.; Hilbrich, R.; Lucken, L.; Rummel, J.; Wagner, P.; Wießner, E. Microscopic Traffic Simulation Using Sumo. In Proceedings of the 2018 21st International Conference on Intelligent Transportation Systems (ITSC), Maui, HI, USA, 4–7 November 2018; pp. 2575–2582.
36. Kobayashi, I.; Tsubota, Y.; Kawashima, H. Eco-driving simulation evaluation of eco-driving within a network using traffic simulation. *WIT Trans. Built Environ.* **2007**, *96*, 741–750.
37. Alfaseeh, L.; Djavadian, S.; Tu, R.; Farooq, B.; Hatzopoulou, M. Multi-Objective Eco-Routing in a Distributed Routing Framework. In Proceedings of the 2019 IEEE International Smart Cities Conference (ISC2), Casablanca, Morocco, 14–17 October 2019; pp. 747–752.
38. Bakibillah, A.S.M.; Kamal, M.A.S.; Tan, C.P.; Hayakawa, T.; Imura, J.I. Fuzzy-tuned model predictive control for dynamic eco-driving on hilly roads. *Appl. Soft Comput. J.* **2021**, *99*, 106875. [CrossRef]
39. Altan, O.D.; Wu, G.; Barth, M.J.; Boriboonsomsin, K.; Stark, J.A. Glidepath: Eco-friendly automated approach and departure at signalized intersections. *IEEE Trans. Intell. Veh.* **2017**, *2*, 266–277. [CrossRef]
40. Yu, M.; Long, J.C. An eco-driving strategy for partially connected automated vehicles at a signalized intersection. *IEEE Trans. Intell. Transp. Syst.* **2022**, *9*, 15780–15793. [CrossRef]